Reactivity of Amino Acid Nucleoside Phosphoramidates: A Mechanistic Quantum Chemical Study

ARTICLE *in* THE JOURNAL OF PHYSICAL CHEMISTRY A · NOVEMBER 2011

Impact Factor: 2.69 · DOI: 10.1021/jp208795f · Source: PubMed

6 AUTHORS, INCLUDING:

Servaas Michielssens
University of Leuven
14 PUBLICATIONS **85** CITATIONS
SEE PROFILE

Munmun Maiti
University of Leuven
5 PUBLICATIONS **20** CITATIONS
SEE PROFILE

Mohitosh Maiti
University of Leuven
13 PUBLICATIONS **79** CITATIONS
SEE PROFILE

Arnout Ceulemans
University of Leuven
252 PUBLICATIONS **4,098** CITATIONS
SEE PROFILE

THE JOURNAL OF PHYSICAL CHEMISTRY A

ARTICLE

pubs.acs.org/JPCA

Reactivity of Amino Acid Nucleoside Phosphoramidates: A Mechanistic Quantum Chemical Study

Servaas Michielssens,*[,†] Munmun Maiti,[†] Mohitosh Maiti,[†] Natalia Dyubankova,[†] Piet Herdewijn,[†] and Arnout Ceulemans[‡]

[†]Laboratory for Medicinal Chemistry—Rega Institute for Medical Research, Katholieke Universiteit Leuven, B-3000 Leuven, Belgium

[‡]Department of Chemistry, Katholieke Universiteit Leuven, B-3001 Leuven, Belgium

ABSTRACT: Recent experimental evidence (Maiti et al. *Chem.—Eur. J.*, submitted) indicates that hydrolysis of nucleoside phosphoramidates is subjected to anchimeric influence by carboxyl moieties in the leaving group but also by the base in the nucleotide. A quantum chemical analysis of these findings is presented. First the intrinsic hydrolysis mechanism is investigated for simplified model compounds, and then both amino acid and nucleoside substituents are included. It is found that hydrolysis is assisted by the α-carboxyl group via formation of a five-membered intermediate and that the barrier for the reaction of this intermediate toward the product state can be influenced by the nucleobase. The adenine base protonated on N3 interacts with the transition state and considerably lowers the barrier for hydrolysis. The influence of several base modifications is explained by calculating the pK_a for protonation on N3.

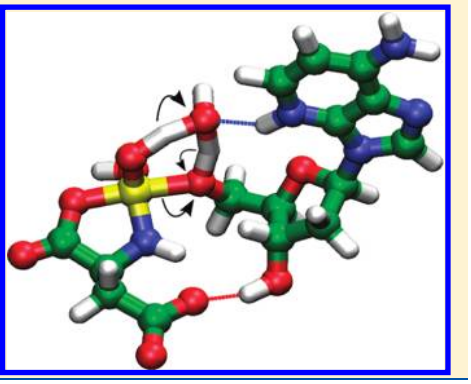

INTRODUCTION

Phosphoramidates have a long history in the scientific literature, but it is only with their use in antiviral strategies in the early 1990s[1−3] that they attracted large attention. The active phosphoramidates are modified nucleotides with different groups linked to the monophosphate via a phosphoramidate linkage. They are part of an antiviral strategy using nucleoside-like inhibitors. The major problem with nucleotide-like viral inhibitors is that administration requires compounds with low charge while the (first) phosphate group is essential for the activity since monophosphorylation by the cellular enzymes is very selective. One strategy to tackle this controversy is shielding the phosphate's charge followed by a transformation in the cell resulting in the monophosphate inhibitor. This method is highly nontrivial since the uptake of the new compounds by the cells must be guaranteed and additionally the compounds need to be selectively transformed. At this point phosphoramidates come into play, since the phosphoramidate linkage appeared to be a successful approach and several nucleoside phosphoramidats (NPs) demonstrated activity.[2,3] The phosphate charge is effectively screened, and thereby the intrusion of those compounds inside the infected cells is assisted. Once inside the cell the NPs are processed to nucleoside monophosphates. The accomplishment of this strategy is proven by the phosphoramidates that reached the clinical trial phase: GS-9140, GS-9131, thymecacin, and stampidine.

Almost two decades after the first attempts to use phosphoramidates as antiviral drugs, Herdewijn et al.[4,5] discovered amino acid nucleoside phosphoramidates (aaNPs) which were direct substrates for polymerases; i.e., they can be incorporated without modification in growing DNA chains using several polymerases. Hence the necessity for cellular processing is totally abolished, and cellular enzymes are completely bypassed. Several modifications were synthesized to optimize their properties.[6−8] The best result was obtained with iminodipropiate as a leaving group.[7] Recently the kinetics of the hydrolysis reaction were studied for a series of aaNPs to determine the influence of the nucleobase and the carboxyl acid groups.[9] An overview of the different aaNPs studied is given in Figure 1. They are similar to the natural nucleotides but with an amino acid linked to the phosphorus via a phosphoramidate bond. Several amino acids were used to look at the influence of α- and β-carboxyl groups. The presence of α-carboxyl groups in the amino acid triggered the hydrolysis of the P−O linkage between phosphate and sugar. Less expected was the finding that the nucleobase has an impact on the hydrolysis rate.[9] A quantum chemical study was launched to explore the different degradation pathways. The present contribution offers a detailed account of the theoretical results, which complement the previous kinetic and NMR study. The aim is to understand the mechanistic influence of the various components as a prerequisite to rationally improve the activity of the aaNPs.

Despite the exponential growth of the work on phosphoramidate, little theoretical work has been done to explore the intrinsic properties of phosphoramidates. In a previous theoretical study[10] the hydrolysis mechanism was compared for *N*-methyl phosphoramidate and methyl phosphate; at present this is extended to *N*,*O*-dimethyl phosphoramidate as a simplified model for aaNP. Next the *N*-methyl is replaced by aspartate to study the

Received: September 12, 2011
Revised: October 31, 2011
Published: November 10, 2011

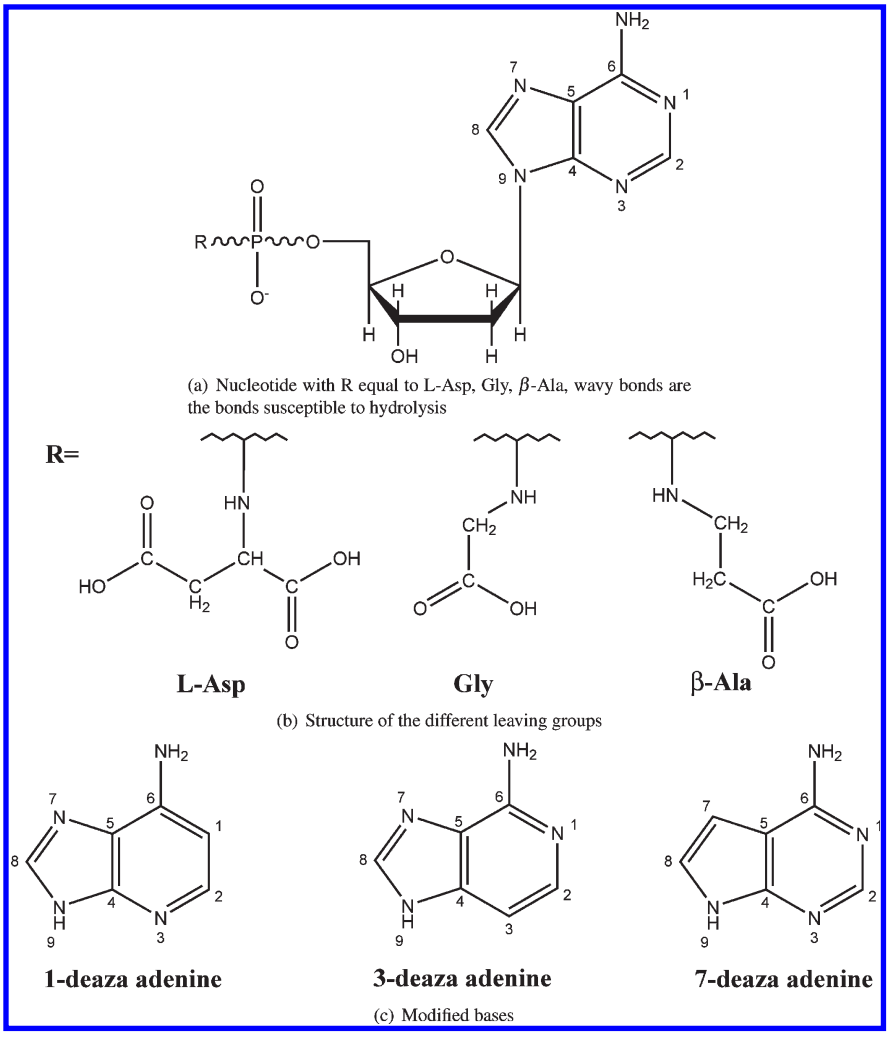

Figure 1. Overview of different bases and leaving groups studied.

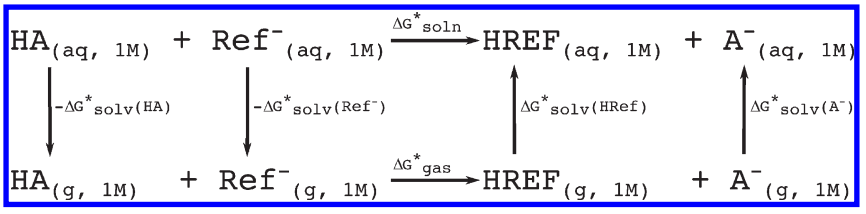

Figure 2. Thermodynamics cycle for the proton exchange method of pK_a calculations.

influence of carboxyl groups on P−O hydrolysis.[9] Subsequently the role of the nucleobase is examined. Experimentally several base modifications were synthesized to test their influence on the hydrolysis rate (Figure 1). The present theoretical analysis provides a mechanistic and structural explanation for the experimental findings. In addition pK_a values were computed for the different protonation sites of the nucleobase explaining the influence of site modifications on the hydrolysis rate.

METHODS

Reaction Mechanisms. All calculations were performed using the Gaussian09 package.[11] Visualization was done with VMD.[12] The structures were optimized using the B3LYP method[13] with DGDZVP[14,15] basis set. All structures were optimized in solvent with the polarizable continuum PCM model using the integral equation formalism variant.[16,17] To compute the free energy of solvation the solvent−solute dispersion and repulsion energy[18,19] and the cavity energy were included.[20] Surface scans of the different molecules used were done by varying the dihedral angles and comparing the energies.

In the reaction pathways every stationary point was checked by frequency analysis. ZPE correction using B3LYP were scaled[21] with a factor of 0.9877. The energy of the B3LYP/DGDZVP optimized structures was corrected doing single point MP2/6-311++G** calculations on them.

Molar energies in tables are reported as follows: ΔE_g is the energy in the gas phase, ΔE_{B3LYP} is the B3LYP/DGDZVP energy

dx.doi.org/10.1021/jp208795f |J. Phys. Chem. A 2012, 116, 644–652

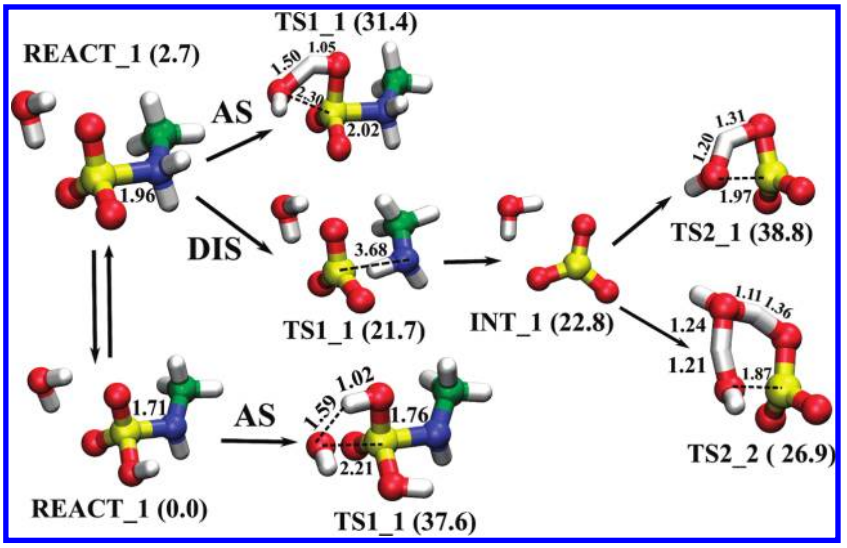

Figure 3. Stationary points on the pathways for the associative and dissociative mechanism of NMP hydrolysis.

with zero point energy correction, and ΔE_{MP2} is the single point MP2/6-311++G** energy with zero point energy correction (using B3LYP/DGDZVP frequencies). $\Delta\Delta G_{aq}$ is the free energy of solvation computed at the B3LYP level, and $\Delta G_{B3LYP_{aq}}$ and $\Delta G_{MP2_{aq}}$ are respectively the B3LYP and MP2 energies including the free energy of solvation. The nomenclature of the stationary points on the reaction pathways is as follows: X_Y_Z, where X is a character referring to the type of mechanism, e.g., D for dissociative and A for associative, Y refers to the type of stationary points (reactant (REACT), intermediate (INT), transition state (TS)), and Z is the number of water molecules involved.

pK_a Calculations. For the pK_a calculations the proton exchange method is applied.[22] The thermodynamic cycle for this method is illustrated in Figure 2. In this cycle the experimental value for the free energy of solvation of the proton is absent, which might otherwise be a source of error. An additional advantage is that the number of charged species is conserved. This leads to a cancellation of errors especially in computing the free energy of solvation. One can maximally profit from cancellation of errors if the reference molecule is similar to the molecule of interest. The pK_a of adenine (3.8)[23] is used as a reference in this work. All compounds differ only by the protonation position or by one nitrogen. When $\Delta G_{soln}{}^*$ is computed the pK_a can be obtained through eq 1.

$$pK_a = \frac{\Delta G_{soln}{}^*}{RT\ln(10)} + pK_a(\mathrm{HRef}) \qquad (1)$$

pK_a(HRef) is the experimental value obtained for the reference compound, in this case adenine. Several methods to determine the different free energies in the thermodynamic cycle were tested. Two different methods are used for the accurate determination of the gas phase free energies, the G4MP2[24] method and the G4 method;[25] both methods perform well and the major difference originates in the treatment of solvation. Five different methods are used to determine the free energy of solvation. The first solvation model is a conductorlike polarizable continuum model (CPCM) using UAKS radii with PBE1PBE/6-31G(d) for which these radii are optimized. The second solvation model is again a CPCM model using UAKS radii with b3lyp/6-311+G(d,p). In the third model UAHF radii with HF/6-31G(d) are used.

Table 1. Relative Energies for Stationary Point for P−N Bond Cleavage in NMP

	ΔE_{B3LYP}	ΔE_{MP2}	$\Delta\Delta G_{aq}$	$\Delta G_{B3LYP_{aq}}$	$\Delta G_{MP2_{aq}}$
Associative Mechanism via $[MeNHPO_3H]^-$					
Without Catalytic H_2O					
REACT_1	0.0	0.0	−52.3	0.0	0.0
AS_TS_1	44.1	42.9	−55.9	40.6	39.4
With Catalytic H_2O					
REACT_2	0.0	0.0	−48.3	0.0	0.0
AS_TS_2	43.3	42.5	−53.3	38.3	37.6
Associative Mechanism via $[MeNH_2PO_3]^-$					
REACT_1	8.2	12.1	−61.8	−1.2	2.7
AS_TS_1	45.9	47.6	−68.6	29.7	31.4
Dissociative Mechanism via $[MeNH_2PO_3]^-$					
Step 1: P−N Bond Dissociation					
DIS_TS1_1	10.3	15.6	−46.3	16.4	21.7
DIS_INT_1	6.3	13.3	−42.9	15.8	22.8
Step 2: Formation of P−O Bond: Attack of Water on Metaphosphate					
Without Catalytic H_2O					
DIS_TS2_1	30.1	36.7	−57.6	32.2	38.8
With Catalytic H_2O					
DIS_TS2_2	20.0	27.9	−59.9	19.0	26.9

In the fourth and fifth models solvation energies use SMD from Truhlar et al.[26] combined with B3LYP/6-311+G(d,p) and B3LYP/6-31G* respectively.

RESULTS AND DISCUSSION

P−N Bond Hydrolysis for Model Compounds: The Effect of Methyl Substitution on Phosphoramidate. *N,O*-dimethyl phosphoramidate (NODP) is an excellent model compound to study P−N bond hydrolysis in L-Asp-dAMP . The Asp and the nucleoside moieties are both replaced by a methyl group and only

dx.doi.org/10.1021/jp208795f |J. Phys. Chem. A 2012, 116, 644–652

the core is preserved; this makes NODP well suited to study the intrinsic properties and hydrolysis mechanisms of NPs. In a preliminary work we studied the simplified *N*-methyl phosphoramidate (NMP) which lacks the monomethyl ester bond.[10] We first resume these previous results on NMP. Now the structures are all optimized in implicit solvent; this in contrast to previous work[10] where only single point solvent corrections were used. In Figure 3 the geometries of the different stationary points for hydrolysis of NMP are given. There are two reactive tautomers of NMP, one with oxygen protonated and the other with nitrogen protonated (OH/NH vs O^-/NH_2^+). Both tautomers are almost equal in energy when solvent effects are considered, as can be seen in Table 1. The tautomer with nitrogen protonated is 8.2 kcal less stable in the gas phase, but solvent effects favor this tautomer by 9.5 kcal/mol, yielding only a small energy difference of −1.2 kcal/mol between both tautomers at the B3LYP level. Both associative and dissociative reaction mechanisms were considered, but for the OH/NH tautomer a dissociative mechanism is impossible since this would require an amide ion as a leaving group, which is a strong base and thus a bad leaving group. Comparing the associative mechanisms it can be seen (Table 1) that the OH/NH tautomer has a lower barrier in vacuum and the order is reversed in solvent. This can be explained by the fact that two oxygens on phosphoramidate carry a negative charge in the case of O^-/NH_2^+, which hinders nucleophilic attack in vacuum, but this hindrance is reduced by the solvent. Note that the mechanism is called associative mechanism because the P−N bond is not fully broken before the P−O bond is formed, but it can also be argued that it is a concerted mechanism, since especially in the O^-/NH_2^+ tautomer, the P−N bond cleavage in the intermediate or transition state is already quite advanced. The lowest barrier can be found for the dissociative mechanism (of the O^-/NH_2^+ tautomer); here the P−N bond is broken before the new P−O bond formation starts. The barrier for the dissociation step is 21.7 kcal/mol, which is remarkably lower than the barrier of 31.4 kcal/mol for the associative mechanism. The highest barrier here is for attack of water on metaphosphate. This can be catalyzed by an extra water molecule that facilitates the proton transfer to phosphate which reduces the barrier from 38.8 to 26.9 kcal/mol. It should be noted here that for the dissociative pathway there is a remarkable difference between the MP2 and B3LYP calculations; for both the dissociative pathway is the lowest in energy, but on the MP2 level of theory the barrier is 7.9 kcal/mol higher. This contrasts with the associative pathway where the difference in barrier is only 1.7 kcal/mol. Overall it can be concluded that a dissociative pathway is expected for NMP.

We now compare these results to our previous work.[10] Here all compounds were optimized in vacuum, and only the OH/NH tautomer was used as a reactant. When comparing the results for the lowest energy pathway of the associative mechanism (AS_TS_2), the barriers in vacuum are similar (37.6 kcal/mol versus 40.5 kcal/mol) . The difference can be explained by the different optimization strategies used. As can be expected the difference in solvent is larger, since here optimization is done in solvent and a lower barrier can be expected. Comparing the result quantitatively it can be seen that this is true (44.2 kcal/mol versus 38.3 kcal/mol). In previous work[10] the dissociative mechanism was considered but starting from the OH/NH tautomer, the first step in the reaction mechanism was a proton transfer from phosphate to nitrogen. To compare the barriers with this work, we compare starting from this intermediate. This comparison gives a

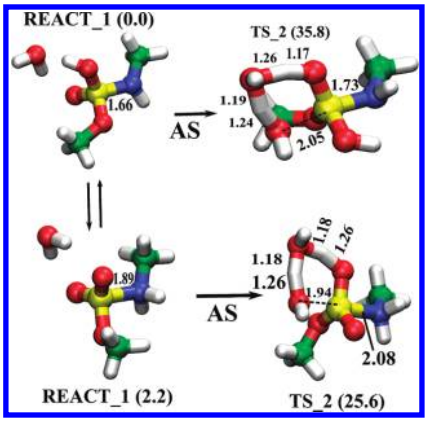

Figure 4. Stationary points on the pathways for the associative and dissociative mechanism of NODP hydrolysis.

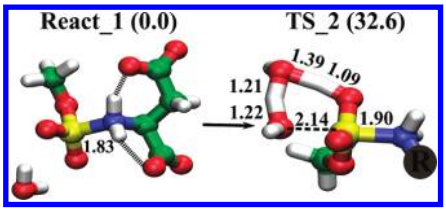

Figure 5. Stationary points for P−N bond hydrolysis in *N*-(methoxyphosphinato)aspartate. In the transition state the carboxyl groups are removed for clarity.

similar picture as for the associative mechanism: a higher barrier in vacuum (22.4 kcal/mol versus 27.9 kcal/mol) and reduced barrier in solvent (35.5 kcal/mol versus 26.9 kcal/mol). Most importantly the same mechanism was inferred.

We now turn to the NODP model, where the presence of the nucleoside is mimicked by a methoxy ester. For NODP there are again two tautomers: a neutral and zwitterionic tautomer (O^-/NH_2^+ vs OH/NH). Comparing the reactants for the zwitterionic tautomers of NODP and NMP, there is a difference in P−N bond length: 1.89 Å versus 1.96 Å; this can be seen comparing Figure 3 and Figure 4. In vacuum the difference is even more pronounced: 1.89 Å versus 2.15 Å. This indicates that the P−N bond is stronger in NODP compared to NPM. This can also explain why the dissociative pathway cannot be found here. It is known[27] that the transition state for unsubstituted phosphoramidate is more dissociative in nature than for monomethyl phosphoramidate; this is on par with our results on NODP and NMP. Again the zwitterionic species is found to be the more reactive one. The transition state includes a catalytic water molecule which lowers the barrier by 5.7 kcal/mol. Overall it can be concluded that methyl substitution shifts the mechanism from dissociative to associative. As a result an associative mechanism is also expected for P−N bond hydrolysis in L-Asp-dAMP.

P−N and P−O Bond Hydrolysis in *N*-(Methoxyphosphinato)-aspartate. *P−N Bond Hydrolysis.* For P−N bond hydrolysis the same mechanism as in NODP is anticipated; this is an associative mechanism via the O^-/NH_2^+ tautomer. The P−N bond length differs from the bond length in NPME: 1.83 Å versus 1.89 Å respectively. This points to a stronger P−N bond. The explanation can be found in the intramolecular interactions (Figure 5). The intramolecular hydrogen bonds of the carboxyl groups to the protonated nitrogen extend the N−H bond length and decrease

dx.doi.org/10.1021/jp208795f |*J. Phys. Chem. A* 2012, 116, 644–652

Table 2. Relative Energies for Stationary Point for P−N Bond Cleavage in NODP

	ΔE_{B3LYP}	ΔE_{MP2}	$\Delta\Delta G_{aq}$	$\Delta G_{B3LYP_{aq}}$	$\Delta G_{MP2_{aq}}$
Associative Mechanism via [$MeNHPO_3HMe$]					
Without Catalytic H_2O					
REACT_1	0.0	0.0	0.1	0.0	0.0
AS_TS_1	39.0	37.9	1.9	40.8	39.7
Associative Mechanism via [$MeNHPO_3HMe$]					
With Catalytic H_2O					
AS_TS_2	34.9	32.9	1.8	37.7	35.8
Associative Mechanism via [$MeNH_2PO_3Me$]					
Without Catalytic H_2O					
REACT_1	14.7	15.6	−13.2	1.3	2.2
AS_TS_1	34.0	35.5	−4.0	29.9	31.3
Associative Mechanism via [$MeNH_2PO_3Me$]					
With Catalytic H_2O					
AS_TS_2	24.5	26.9	−2.4	23.0	25.6

Table 3. Relative Energies for Stationary Point for P−N Bond Cleavage in *N*-(Methoxyphosphinato)aspartate

	ΔE_{B3LYP}	ΔE_{MP2}	$\Delta\Delta G_{aq}$	$\Delta G_{B3LYP_{aq}}$	$\Delta G_{MP2_{aq}}$
Without Catalytic H_2O					
REACT_PN_1	0.0	0.0	−151.0	0.0	0.0
AS_TS_1	45.4	43.2	−160.0	36.3	34.1
With Catalytic H_2O					
REACT_PN_2	0.0	0.0	−150.5	0.0	0.0
AS_TS_2	38.9	38.8	−156.6	32.8	32.6

the P−N bond length. Comparing the geometry of the transition state in Figure 4 and Figure 5, it can be seen that in the former the reaction is more evolved toward the product state: the P−O bond length is 0.2 Å shorter and the P−N bond length 0.18 Å longer. This is also reflected in the barrier (Table 2 versus Table 3): the barrier for NODP hydrolysis is 7 kcal/mol lower than in the case of *N*-(methoxyphosphinato)aspartate. This effect is even more pronounced when solvent effects are not considered (difference of 11.9 kcal/mol).

P−O Bond Hydrolysis in N-(methoxyphosphinato)aspartate. The kinetic experiments by Maiti et al.[9] clearly indicate that P−O bond hydrolysis occurs only when there is an α-carboxyl group. Reaction rates and product distribution for dAMP were compared with different leaving groups. For a β-alanine leaving group, there is no α-carboxyl group and only P−N bond hydrolysis occurs. With aspartic acid and glycine as leaving group, P−O hydrolysis occurs. It is anticipated that the formation of a five-membered ring by attack of the α-carboxyl group on phosphate facilitates the P−O bond hydrolysis. For this compound the O^-/NH_2^+ tautomer is more stable than the OH/NH tautomer. But all the P−O bond hydrolysis reactions occur via the OH/NH tautomer, since in all the mechanisms the P−N bond must be in an equatorial position in the intermediate, which is not possible for the O^-/NH_2^+ tautomer. In Table 4 different mechanisms for P−O bond hydrolysis are considered. C5A points to a cyclic

Table 4. Relative Energies for Stationary Point for P−O Bond Cleavage in *N*-(Methoxyphosphinato)aspartate

	ΔE_{B3LYP}	ΔE_{MP2}	$\Delta\Delta G_{aq}$	$\Delta G_{B3LYP_{aq}}$	$\Delta G_{MP2_{aq}}$
Direct Mechanism					
Without Catalytic H_2O					
A_TS1_1	51.0	48.5	−50.8	45.6	43.1
A_INT_1	36.9	33.5	−51.7	30.6	27.2
With Catalytic H_2O					
A_TS1_2	47.9	45.5	−49.8	41.0	38.5
Autocatalysis: Five-Membered Ring					
Without Catalytic H_2O					
REACT_PN	0.0	0.0	−48.3	0.0	0.0
REACT_PO	9.9	7.6	−52.4	5.8	3.5
C5A_TS1	28.1	27.6	−55.5	21.0	20.4
C5A_INT	18.5	17.0	−52.0	14.7	13.3
C5A_TS2	36.8	35.3	−49.4	35.7	34.3
With Catalytic H_2O					
C5A_TS1_1	23.9	24.1	−54.4	14.9	15.2
C5A_INT_1	17.9	17.3	−51.3	12.0	11.4
C5A_TS2_1	35.7	34.4	−55.6	25.5	24.3
Autocatalysis: Six-Membered Ring					
Without Catalytic H_2O					
C6A_TS1	28.9	28.0	−54.4	22.8	21.9
C6A_INT	23.1	21.8	−50.7	20.7	19.3
C6A_TS2	37.4	35.6	−47.1	38.6	36.9
With Catalytic H_2O					
C6A_TS2_1	38.5	37.2	−53.3	30.7	29.4

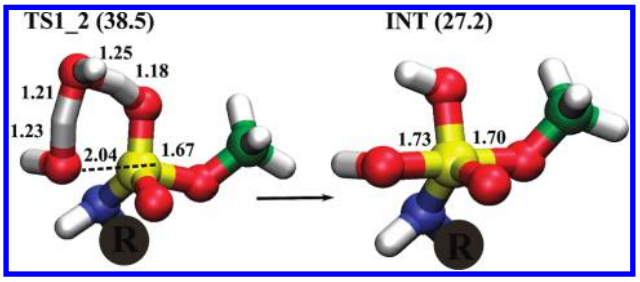

Figure 6. Stationary points for P−O bond hydrolysis via a direct mechanism in *N*-(methoxyphosphinato)aspartate.

structure with a five-membered ring structure and C6A to a six-membered ring, where the A refers to the associative nature of the mechanism. The direct mechanism (Figure 6) is an associative mechanism where water attacks directly on the phosphate. The attacking water molecule is on the opposite side of the methanol leaving group, and the proton transfer occurs via a catalytic water molecule. A pentacoordinated phosphorus is formed after this step. The barrier to form this pentacoordinated phosphorus via the direct mechanism is 38.5 kcal/mol; this is the barrier including solvent and including a catalytic water molecule. As an alternative this pentacoordinated phosphorus can be formed by attack of the α- or β-carboxyl group, to form a five-membered or six-membered ring intermediate, respectively. We refer to this

dx.doi.org/10.1021/jp208795f | J. Phys. Chem. A 2012, 116, 644–652

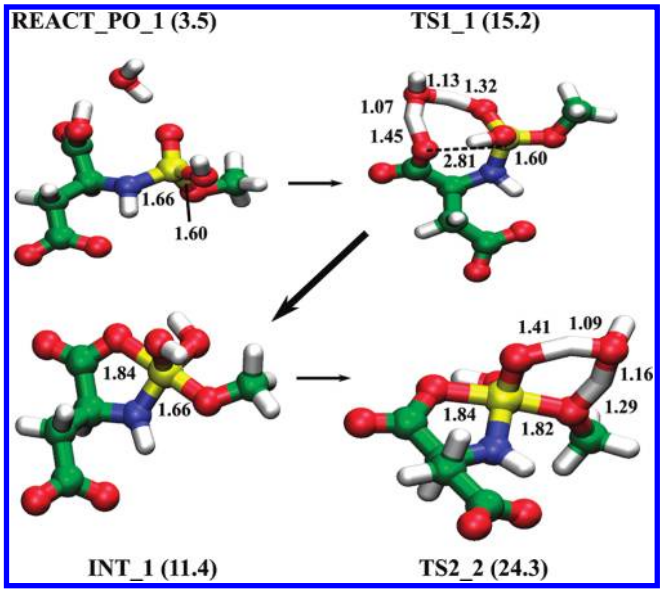

Figure 7. Stationary points for P−O bond hydrolysis via a cyclic intermediate in *N*-(methoxyphosphinato)aspartate.

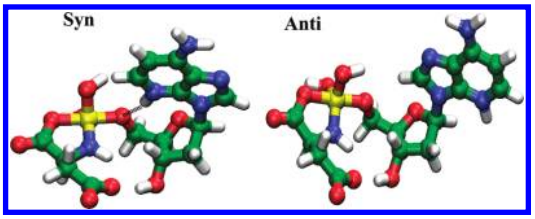

Figure 8. Syn and anti conformation of the base in L-Asp-1-deaza-dAMP.

mechanism as autocatalysis. Comparing the five-membered to the six-membered ring intermediate in Table 4 it can be seen that the C5A_int is 6 kcal/mol more stable than C6A_INT and 13.9 kcal/mol than A_INT in the direct mechanism (comparing the intermediate states without catalytic water molecule). The same trend can be found in the barrier to form this intermediate. From this it can be concluded that a five-membered ring intermediate is expected for P−O bond hydrolysis. The details of the geometries in the pathway for P−O bond hydrolysis via the five-membered ring intermediate are given in Figure 7. As in the direct mechanism there is an important role for a catalytic water molecule to assist the proton transfer; this lowers the barrier by 9 kcal/mol. The P−O distance in the C5A_TS1_1 is 2.81 Å compared to 2.04 Å for A_TS1_2 in the absence of the anchimetric assistance of the carboxyl groups. In the latter the formation of the P−O bond is much more advanced in the transition state. The proton has largely departed from the carboxyl group; the distance is 1.45 Å and is mainly located on the intermediate water molecule in C5A_TS1_1, while in A_TS1_2 the protons are much more intermediate between the oxygens (Figure 6). Several theoretical studies report on the formation of this five-membered ring intermediate for phosphoramidates where an α-carboxyl group is present. These include *N*-phosphorylaspartic acid[28] and diisopropoxyl *N*-phosphoryl L-alanine.[29] In the study on *N*-phosphorylaspartic acid[28] the formation of peptides from phopshoryl amino acids is investigated. The model system differs by one extra methoxy group on the phosphorus, and both α- and β-carboxyl groups are protonated. The comparison is interesting since the first reaction step is also the formation of a cyclic intermediate. Both the possibility of five-membered and six-membered ring are considered with the same conclusion as in this work. A quantitative comparison is difficult since the methods used are different and the model compounds are not exactly the same, but still the barriers found are similar if the barrier is considered starting from the OH/NH tautomer (15.2 kcal/mol vs 13.16 kcal/mol), and both studies indicate the preferential formation of a five-membered ring. Since in ref 28 the P−O bond hydrolysis was not investigated, the second and most important step in our hydrolysis mechanism cannot be compared. For diisopropoxyl *N*-phosphoryl L-alanine[29] also catalytic water is included in the transition state for the formation of the five-membered ring. A barrier of 9.9 kcal/mol was found compared to the OH/NH tautomer; this is very similar to the present result of 11.7 kcal/mol (when comparing to the same tautomer, difference between REACT_PO and C5A_TS1_1). Again the second step required for hydrolysis was not considered. When the five-membered intermediate is formed the P−O bond still needs to be hydrolyzed, and protonation of the leaving group is required for this. This step in the hydrolysis reaction has been studied for *N*-(*O*,*O*-dimethyl)phosphoryl amino acids,[30] and a barrier of 29.9 kcal/mol was reported but no detailed geometries. Comparing to our result without catalytic water and taking into account that the barrier reported for *N*-(*O*,*O*-dimethyl)-phosphoryl amino acid was compared to the REACT_PO tautomer, exactly the barrier is found here. The role of catalytic water was not considered, and it will be shown here that its role is crucial. Catalytic water reduces the barrier by 10 kcal/mol as listed in Table 4. The detailed geometry is shown in Figure 7. Note that an interchange mechanism, where the attack of water occurs simultaniously with the proton transfer to the leaving group, is not possible since here in the transition state there are six groups around phosphorus which results in a high barrier.

Experimentally it was also noted that the presence of an α- and β-carboxyl group enhances the rate of P−O bond hydrolysis more than the presence of only an α-carboxyl group. This was observed comparing the reaction rates for a glycine leaving group to an aspartic acid leaving group.[9] The calculations do not point to an active role of the β-carboxyl group in the mechanism, but a structural role might be anticipated. The presence of the hydrogen bond between the β-carboxyl group and the NH places the α-carboxyl group in the correct position for attack on the phosphorus (Figure 7). The possibility of this interaction was also shown in the NMR experiments.[9]

Influence of the Nucleobase on the Hydrolysis. P−O bond hydrolysis is found to be influenced by the nucleobase. Maiti et al.[9] compared several bases (shown in Figure 1) and observed the following ordering (fast to slow hydrolysis): 1-deaza-adenine > 7-deaza-adenine > adenine > thymidine ≥ 3-deaza-adenine. Especially 1-deaza-adenosine enhances the rate of P−O bond hydrolysis. The experiments were performed in acidic pH where N3 of adenosine is protonated. From the above calculations on *N*-(methoxyphosphinato)aspartate, it was found that the highest barrier in the preferred hydrolysis pathway is the C5A_TS2_2 transition state. To enhance the rate this barrier needs to be reduced. Since we are interested in TS2, we will consider the barrier starting from the intermediate toward TS2 and how this can be influenced by the base. For the base to have an influence it must be in a syn conformation (Figure 8). The first question that needs to be addressed is the possibility for a syn conformation of

dx.doi.org/10.1021/jp208795f |*J. Phys. Chem. A* 2012, 116, 644–652

the base in the intermediate. To address this, the full L-Asp-1-deaza-dAMP was considered and the energies for syn and anti conformation were computed (Table 5). Both are almost equal in energy; hence it can be concluded that a syn conformation is an acceptable conformation here. This was also seen in the NMR experiments[9] where several measurements indicated a significant population of the syn conformer in Asp-1deaza-dAMP . It should be noted that especially on the MP2 level the intramolecular basis set superposition error differs for the syn and anti conformation. This is easily understood since the overlap between the basis functions of the sugar and base is clearly larger in the syn conformation. The basis set superposition error was computed here by dividing the molecule in two parts: the base and the rest. The syn conformation is stabilized by a hydrogen bond between N3−H and the 5′ oxygen of the sugar. The heavy atom distance is 3.05 Å and the angle is 168°, which points to a fairly strong hydrogen bond.

Table 5. Relative Energy for Syn versus Anti in the Intermediate State

	ΔE_{B3LYP}	ΔE_{MP2}	$E_{CPB3LYP}$	E_{CPMP2}	$\Delta\Delta G_{aq}$	$\Delta G_{B3LYP_{aq}}$	$\Delta G_{MP2_{aq}}$
syn	0.0	0.0	−3.0	−12.3	−45.8	0.0	0.0
anti	13.7	16.3	−2.3	−9.9	−59.0	−0.6	1.9

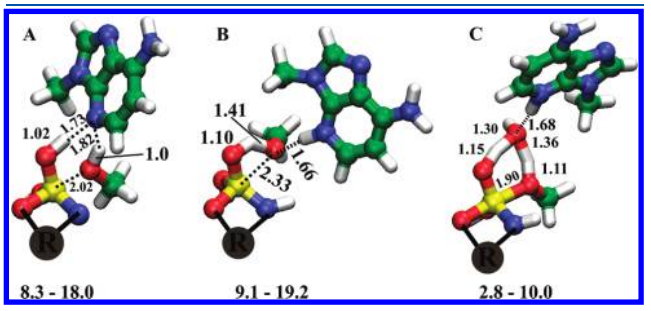

Figure 9. Different roles for the nucleobase in the catalysis. The numbers within parentheses are B3LYP energies in vacuum and solvent with respect to the intermediate. In A, the base takes the role of proton shuttle. In B, the hydrogen bond stabilizes the leaving group. In C, the base has a hydrogen bridge to the catalytic water molecule which pushes the reaction to the product side and lowers the barrier.

Table 6. Influence of the Nucleobase in the Full Nucleotide

	ΔE_{B3LYP}	ΔE_{MP2}	$\Delta\Delta G_{aq}$	$\Delta G_{B3LYP_{aq}}$	$\Delta G_{MP2_{aq}}$
int	0.0	0.0	−29.6	0.0	0.0
ts	6.4	6.3	−25.9	10.1	10.0

To screen different roles for the base, the sugar was removed to allow full flexibility of the base positioning. Afterward the interesting mechanisms are investigated with the full L-Asp-1-deaza-dAMP. In the screening phase B3LYP energies with and without solvation were used (energies are relative to the intermediates, and for model without the base this barrier was 17.1 kcal/mol in vacuum and 12.9 kcal/mol in water). Three possibilities were considered, which are shown in Figure 9. In the first mechanism (A) the base replaces water as a proton shuttle from phosphoramidate toward the methanol leaving group. In vacuum this drastically reduces the barrier to 8.3 kcal/mol, but considering solvent effect the barrier is 18.0 kcal/mol. The second possibility (B) is that the hydrogen bond stabilizes the leaving group facilitating its departure. A similar effect is observed in vacuum; here the barrier is reduced to 9.1 kcal/mol, but the advantage is again removed by considering solvent effects (19.1 kcal/mol). The most spectacular effect is seen if the base is forming a hydrogen bond with a catalytic water molecule (C). This reduces the barrier in vacuum to 2.8 kcal/mol and in solvent to 10.0 kcal/mol. To verify this mechanism, it was also studied in the full L-Asp-1-deaza-dAMP. The barrier is given in Table 6; in vacuum the barrier changed to 6.4 kcal/mol and in water to 10.1 kcal/mol on the B3LYP level (results on the MP2 level differ by only 0.1 kcal/mol). This is a spectacular lowering of the barrier in vacuum and a mild reduction of the barrier in solvent. To understand this effect, the geometries of the transition states in Figure 9 C and Figure 7 are

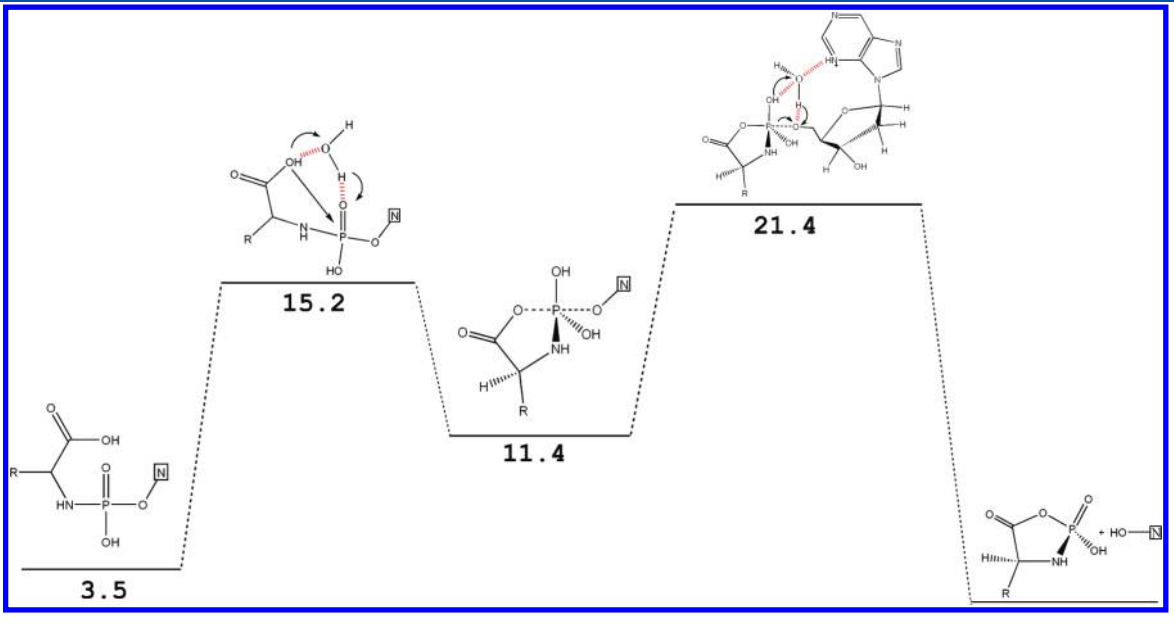

Figure 10. Schematic representation of the preferred pathway for P−O bond hydrolysis in L-Asp-1-deaza-dAMP. First a five-membered ring intermediate is formed, and this is hydrolyzed with assistance of the protonated base. The hydrogen bond network used for the proton transfer steps is indicated red. Note that a catalytic water molecule is involved in both transition states.

dx.doi.org/10.1021/jp208795f |J. Phys. Chem. A 2012, 116, 644–652

Table 7. pK_a Results Using the G4MP2 or G4 Method for the Gas Phase Calculations Combined with Five Different Solvent Models[a]

	G4MP2					G4					
	solv1	solv2	solv3	solv4	solv5	solv1	solv2	solv3	solv4	solv5	exp.
adenine N1	–	–	–	–	–	–	–	–	–	–	3.8[23]
adenine N3	1.7	1.9	1.8	2.2	2.1	1.6	1.9	1.7	2.2	2.1	–
1-deaza N3	3.4	3.4	2.8	5.0	5.0	3.5	3.5	2.9	5.1	5.1	4.6[9]
3-deaza N1	6.6	6.5	6.3	7.6	7.8	6.7	6.6	6.4	7.9	7.9	7.5[9]
7-deaza N1	5.6	5.2	5.8	5.6	5.4	5.7	5.3	5.9	5.7	5.5	4.7[9]
7-deaza N3	3.6	3.7	3.7	4.3	4.3	3.6	3.7	3.7	4.4	4.3	–

[a] Solv1 = CPCM with PBE1PBE/6-31G(d); solv2 = CPCM with PBE1PBE/6-31G(d); solv3 = CPCM with HF/6-311+G(d,p); solv4 = SMD with B3LYP/6-311+G(d,p); solv5 = SMD with B3LYP/6-31G(d); more details are given in the text. Note that for adenine protonation on N1 only the experimental value is given since this is used as a reference compound.

compared. It can be seen that the reaction with the base is more evolved toward the product state: the P−O distance is 0.08 Å longer and the proton is 0.18 Å closer to the methanol leaving group. From this it can be inferred that hydrogen bridge of the base to the catalytic water molecule pushes the reaction further to the product state and by this lowers the barrier. The proposed mechanism explains the high reactivity of the 1-deaza-adenine compound and the low reactivity of the 3-deaza-adenine and thymidine compounds where the relevant hydrogen bridge cannot be formed. The intermediate activities for the 7-deaza-adenine and unsubstituted adenine are less clear and require detailed considerations of the preferential protonation sites, as discussed in the next section.

Overall we can conclude for the hydrolysis of the P−O bond in L-Asp-1-deaza-dAMP that the preferred pathway is a two step process. This includes first the formation of the five-membered ring system intermediate via attack of the α-carboxyl group of the amino acid moiety. The second step is the departure of the nucleoside moiety on the pentacoordinated phosphorus with assistance of the protonated nucleobase. This process is summarized in Figure 10.

pK_a Calculations. Both 7-deaza-adenine and adenine can be protonated on the N3 position, but the experimental results showed that N1 is the preferential protonation position for both. It might be anticipated that while N1 protonation is dominant, the reactive species for P−O bond hydrolysis is with N3 protonated. This hypothesis can be tested by computing the pK_a values for protonation of N3 in the 1-deaza and 7-deaza compounds. From the experimental reactivity one would expect that pK_a(7-deaza-adenine, N3) > pK_a(adenine, N3) if this hypothesis is valid. In Table 7 the results of the pK_a calculations are shown. There is little difference in the results using the G4MP2 or G4 method for the gas phase energies; the dominant influence comes from the solvent model. The SMD model of Truhlar et al. with B3LYP/6-311+G(d,p) performs the best for the test set with the largest deviation of 0.7 pK_a units for 7-deaza-adenine. The computational result is also systematically higher than the experimental result. The pK_a for N3 protonation in 7-deaza-adenine was found to be 4.2 and for N3 in adenine 2.1. This is on par with the hypothesis that the higher reactivity of 7-deaza-adenine over adenine can be explained by the higher proportion of N3 protonation.

CONCLUSION

By studying methyl substitution on phosphoramidate in model compounds it was found that an associative mechanism can be expected for P−N bond hydrolysis in L-Asp-dAMP. Expansion of this model by including the Asp moiety confirmed this conclusion. The experimental findings that P−O bond hydrolysis can only be found if an α-carboxyl group is present are explained. The intramolecular catalysis via a five-membered ring of this group reduced the barrier by more than 10 kcal/mol. However, without intramolecular catalysis the barrier for P−N bond hydrolysis is lower than for P−O bond hydrolysis. This order is reversed in the presence of an α-carboxyl group. Moreover, the role of the nucleobase and especially the remarkable role of 1-deaza-adenosine is explained by a syn conformation of the base with hydrogen bonding of the protonated base to the catalytic water molecule in transition state. This pushes the transition state toward the products and reduces the barrier. The entire mechanism for P−O bond hydrolysis is summarized in Figure 10.

Additionaly pK_a values for the different protonation sites are predicted and are on par with the hypothesis that the hydrolysis rate is proportional to the pK_a of the N3 nitrogen in the base. When N3 is preferentially protonated (for 1-deaza adenine), hydrolysis is faster and the rate decreases when the pK_a of N3 protonation drops (for 7-deaza and 3-deaza).

This work provides a mechanistic explanation for the experimental observations comparing the hydrolysis of some promising aaNPs, but the data provided can also be used to test the mechanism that is proposed, e.g., by varying the pK_a of the N3 position using halogen substitution on the nucleobase. Modifications with lower pK_a could be used to stabilize the aaNPs.

AUTHOR INFORMATION

Corresponding Author

*E-mail: servaas.michielssens@chem.kuleuven.be.

ACKNOWLEDGMENT

This work has been supported by the Fund for Scientific Research-Flanders (FWO).

REFERENCES

(1) McGuigan, C.; Tollerfield, S.; Riley, P. *Nucleic Acids Res.* **1989**, *17*, 6065–6075.

(2) Mehellou, Y.; Balzarini, J.; McGuigan, C. *ChemMedChem* **2009**, *4*, 1779–1791.

(3) Cahard, D.; McGuigan, C.; Balzarini, J. *Mini-Rev. Med. Chem.* **2004**, *4*, 371–381.

(4) Adelfinskaya, O.; Herdewijn, P. *Angew. Chem., Int. Ed.* **2007**, *46*, 4356–4358.
(5) Adelfinskaya, O.; Terrazas, M.; Froeyen, M.; Marliere, P.; Nauwelaerts, K.; Herdewijn, P. *Nucleic Acids Res.* **2007**, *35*, 5060–5072.
(6) Giraut, A.; Herdewijn, P. *ChemBioChem* **2010**, *11*, 1399–1403.
(7) Giraut, A.; ping Song, X.; Froeyen, M.; Marliere, P.; Herdewijn, P. *Nucleic Acids Res.* **2010**, *38*, 2541–2550.
(8) Zlatev, I.; Giraut, A.; Morvan, F.; Herdewijn, P.; Vasseur, J.-J. *Bioorg. Med. Chem.* **2009**, *17*, 7008–7014.
(9) Maiti, M.; Michielssens, S.; Dyubankova, N.; Maiti, M.; Lescrinier, E.; Ceulemans, A.; Herdewijn, P. *Chem.—Eur. J.* Submitted.
(10) Michielssens, S.; Trung, N. T.; Froeyen, M.; Herdewijn, P.; Nguyen, M. T.; Ceulemans, A. *Phys. Chem. Chem. Phys.* **2009**, *11*, 7274–7285.
(11) Frisch, M. J. et al. *Gaussian 09*, revision A.1; Gaussian, Inc.: Wallingford, CT, 2009.
(12) Humphrey, W.; Dalke, A.; Schulten, K. *J. Mol. Graphics Modell.* **1996**, *14*, 33–39.
(13) Becke, A. D. *J. Chem. Phys.* **1993**, *98*, 5648–5652.
(14) Godbout, N.; Salahub, D. R.; Andzelm, J.; Wimmer, E. *Can. J. Chem.* **1992**, *70*, 560–571.
(15) Sosa, C.; Andzelm, J.; Elkin, B. C.; Wimmer, E.; Dobbs, K. D.; Dixon, D. A. *J. Phys. Chem.* **1992**, *96*, 6630–6636.
(16) Miertus, S.; Scrocco, E.; Tomasi, J. *Chem. Phys.* **1981**, *55*, 117–129.
(17) Mennucci, B.; Tomasi, J. *J. Chem. Phys.* **1997**, *106*, 5151–5158.
(18) Floris, F.; Tomasi, J. *J. Comput. Chem.* **1989**, *10*, 616–627.
(19) Floris, F.; Tomasi, J.; Ahuir, J. *J. Comput. Chem.* **1991**, *12*, 784–791.
(20) Pierotti, R. *Chem. Rev.* **1976**, *76*, 717–726.
(21) Andersson, M. P.; Uvdal, P. *J. Phys. Chem. A* **2005**, *109*, 2937–2941.
(22) Ho, J.; Coote, M. L. *Theor. Chem. Acc.* **2010**, *125*, 3–21.
(23) Kazimierczuk, Z.; Vilpo, J.; Seela, F. *Helv. Chim. Acta* **1992**, *75*, 2289–2297.
(24) Curtiss, L. A.; Redfern, P. C.; Raghavachari, K. *J. Chem. Phys.* **2007**, *127*.
(25) Curtiss, L. A.; Redfern, P. C.; Raghavachari, K. *J. Chem. Phys.* **2007**, *126*, 111–119.
(26) Marenich, A. V.; Cramer, C. J.; Truhlar, D. G. *J. Phys. Chem. B* **2009**, *113*, 6378–6396.
(27) Lonnberg, T.; Ora, M.; Lonnberg, H. *Mini-Rev. Org. Chem.* **2010**, *7*, 33–43.
(28) Chen, Z.; Tan, B.; Li, Y.; Zhao, Y.; Tong, Y.; Wang, J. *J. Org. Chem.* **2003**, *68*, 4052–4058.
(29) Tan, B.; Lee, M.; Cui, M.; Liu, T.; Chen, Z.; Li, Y.; Ju, Y.; Zhao, Y.; Chen, K.; Jiang, H. *Comp. Theor. Chem.* **2004**, *672*, 51–60.
(30) Li-Ming, Q.; Shu-Xia, C.; Xiao-Yang, Z.; Ruo-Yu, L.; Ji-Hong, L.; Jian-Sha, L.; Yu-Fen, Z. *Chin. J. Chem.* **2007**, *25*, 1559–1562.